A New Augmented RISE Feedback Controller for Pick-and-Throw Applications with PKMs

Ghina Hassan, Ahmed Chemori, Marc Gouttefarde, Maher El Rafei, Clovis Francis, Pierre-Elie Hervé, Damien Sallé

A New Augmented RISE Feedback Controller for Pick-and-Throw Applications with PKMs

G. Hassan [*,**] **A. Chemori** [*] **M. Gouttefarde** [*] **M. El Rafei** [**]
C. Francis [****] **P.E. Hervé** [***] **D. Sallé** [***]

[*] *LIRMM, Univ Montpellier, CNRS, Montpellier, France (e-mail: ghina.hassan, ahmed.chemori, marc.gouttefarde@lirmm.fr)*
[**] *CRSI, Lebanese University, Faculty of Engineering, Beirut, Lebanon (e-mail: maher.elrafei@ul.edu.lb)*
[***] *TECNALIA, Basque Research and Technology Alliance (BRTA), San Sebastian, Spain (e-mail: pierre-elie.herve, damien.salle@tecnalia.com)*
[****] *MSMP-EA7350, Arts et Métiers ParisTech de Châlons en Champagne, Châlons en Champagne, France. (e-mail: Clovis.francis@ensam.eu)*

Abstract: Most of the current industrial applications (like food packaging, waste sorting, machining, etc.) use parallel kinematic manipulators (PKMs) owing to their high speed and accuracy. However, parallel robots are exposed to highly nonlinear dynamics, time-varying parameters and uncertainties, especially in those applications. Considering all these issues, the synthesis of advanced and robust control schemes for PKMs is considered a challenging task. A new control scheme based on the Robust Integral of the Sign of the Error (RISE) control scheme is proposed in this work. A revision of the standard RISE control law is proposed by considering, in the control loop, a compensation term computed from the dynamic model of the robot, the measured and the desired trajectories, and the tracking error. In addition, we propose to extend the resulting controller with a nonlinear feedback function to compensate for the errors resulting from using the desired trajectories instead of the measured ones in the dynamic compensation term. The proposed control contribution can compensate for PKM parameter uncertainties and high nonlinearities as well as improve the robustness of the standard RISE controller. Numerical simulations have been conducted on a parallel robot, called T3KR, in a pick-and-throw task under different operating conditions to confirm the effectiveness of the proposed control scheme.

Keywords: RISE feedback control, model-based robust control, parallel kinematic manipulator, pick-and-throw, numerical simulations.

1. INTRODUCTION

Parallel Kinematic Manipulators (PKMs) will, in a near future, be increasingly used in industries due to their high dynamics, rigidity, high accuracy and high payload-to-weight ratio (Natal et al., 2014). A parallel robot is generally defined as follows (Merlet, 2006): "A parallel kinematic manipulator is a structure whose moving platform is connected to a fixed base by several independent kinematic chains". Given the aforementioned advantages, PKMs have been widely applied in various applications. For example, they have been used as a flight simulator (Stewart, 1965), in the packaging industry (Clavel, 1990), in medical applications (Dalvand and Shirinzadeh, 2012), in machining tasks (Escorcia-Hernández et al., 2020b), in high-speed handling (Shang and Cong, 2009) and as haptic devices (Grange et al., 2001). In the last few years, they have been used in selective waste sorting, alongside the conventional sorting machines, to increase the purity of streams by removing the unwanted material not selected by the machines. One example is the ABB's Delta robot used as the basis of a sorting robot adopting the pick-and-place (P&P) technique BHS (2018). Recently, the pick-and-throw (P&T) approach has been applied in waste industry aiming to increase the productivity of a PKM (Raptopoulos et al., 2020).

Indeed, parallel manipulators are well known for their unfavorable nonlinearities, abundant modeling uncertainties, external disturbances, and parameter variations (i.e., payload), especially in high-speed industrial applications. In order to achieve better output trajectory tracking despite all of the above challenges, a controller must be robust enough to counteract external disturbances as well as rich in dynamic model knowledge to compensate for system uncertainties and nonlinearities. RISE feedback control, developed by Xian (Xian et al., 2004), is a good candidate for the control of highly nonlinear uncertain dynamical systems. It is a continuous nonlinear control strategy based on the integral of the sign function in terms of the tracking error ensuring disturbances rejection. It is a non-model-based controller that can guarantee a semi-global asymptotic tracking under limited assumptions on the system and the external disturbances. RISE control strategies known by their robustness and disturbance rejection ability were successfully implemented in various real-time applications (Feemster, 2014; Yao et al., 2014). Moreover, the high efficiency of RISE control schemes has been proved experimentally on different robotic applications such as Autonomous Underwater Vehicle (AUV) (Fischer et al., 2011), exoskeleton devices (Sherwani et al., 2020), rigid parallel manipulator (Escorcia-Hernández et al., 2020b) and cable-driven parallel robots (Hassan et al.,

2020). The RISE-based controllers show in the many researches work a high performance compared to standard RISE control law. For instance, in (Bennehar et al., 2018), a RISE-based adaptive control has been proposed as a solution for the control problem of PKMs. It consists in adding model-based adaptive feedforward term to the control loop in order to compensate for parameter variations. Moreover, a Time-Varying RISE-based Control consists in replacing the static feedback gains by nonlinear ones has been proposed and validated experimentally on a parallel manipulator (Saied et al., 2019). In (Escorcia-Hernández et al., 2020a), a RISE feedback controller has been extended by an adaptive feedforward compensation term based on B-Spline Neural Networks (BSNNs) to improve tracking performance of PKMs.

RISE and RISE-based control strategies show, in different applications, significant performance and robustness against disturbances and uncertainties. Therefore, the improvement of this controller attracts the attention of many researchers. The RISE feedback control law is a non-model based controller that depends only on system states, which can lead to low performance in the presence of large uncertainties and hard nonlinearities. Enriching the control loop of original RISE controller by a compensation term based on the dynamic model and the system errors has the potential to improve the performance by accommodating more uncertainties and variations in the dynamic parameters.

In most industrial applications, non-model based control strategies are applied due to their simplicity and ease of implementation. However, as mentioned above, PKMs are often subject to dynamic nonlinearities, uncertainties, parameter variations, external disturbances, etc. Accordingly, non-model-based controllers may lead to poor performance and even instability when operating at critical conditions (e.g. high speed applications, payload changes). Many research works show over the last decades that enriching a controller with knowledge on the manipulator dynamics can compensate for nonlinearities and parameter uncertainties, especially for high-order nonlinear systems (Kelly et al., 2006; Slotine et al., 1991; Ren et al., 2007). Therefore, different model-based controllers have proposed and implemented on PKMs, such as PD with desired gravity compensation (Kelly, 1997), computed torque (CT) control which uses full knowledge of the nonlinear system dynamics (Codourey, 1998) and augmented PD (APD) where the dynamic term depends on both, the desired and measured states (Shang et al., 2009). Furthermore, an extended model-based adaptive feedforward control $\mathscr{L}_1$ has been developed to control mechanical manipulators (Bennehar et al., 2015). A model predictive control (MPC) is designed and implemented on a redundantly actuated parallel robot to improve tracking capability and robustness under disturbances and parameter variations (Wen et al., 2016).

In this paper, a revision of the original RISE feedback law is performed by augmenting its control loop with a nonlinear dynamic compensation term. This term is computed based on a combination of the dynamic parameters of the controlled system, which is a PKM in our study, its state errors, and the measured and desired trajectories. In addition, the resulting controller is extended by an auxiliary nonlinear feedback term to account for the errors that occur by replacing the actual trajectories (specifically the actual velocities and accelerations), in the dynamic compensation term, with the desired trajectories. Numerical simulations are carried out in P&T scenarios with a PKM under different operating conditions (i.e., payload changes, different speeds) to demonstrate the performance improvement and enhancement provided by the proposed control scheme.

The rest of this paper is organized as follows: In Section 2, the description and modeling of T3KR PKM are presented. The background on the RISE control scheme is detailed in Section 3. Section 4 is dedicated to the proposed contribution on RISE control. The obtained numerical simulation results are presented and discussed in Section 5. Section 6 concludes this paper and presents future work.

2. T3KR PKM: DESCRIPTION AND MODELLING

This section describes the design of the mechanical structure of T3KR robot with its kinematic and dynamic model.

2.1 Description and kinematics of T3KR PKM

T3KR is a "Pick-and-Place" PKM, developed in collaboration between Tecnalia, LIRMM and SATT AxLR. This robot is designed to be as economical in footprint as possible (i.e. all its geometrical parameters are optimized). It consists of four driven kinematic chains connected to a common mobile platform. Each kinematic chain is a series arrangement of a revolute actuator, a rearm and a forearm (composed of two parallel rods forming a parallelogram). The forearms are connected, on their first side, to the rearms by passive spherical joints and linked on their other side to the mobile platform by means of the same aforementioned joints (as shown in Fig. 1). This design allows the end-effector to have five Degrees-of-Freedom (DOFs): three translations denoted by x,y,z and the rotation ψ pf the mobile platform around the z-axis are provided by the four actuated arms. In addition, the rotation ϕ of the end-effector around the z-axis is provided by an actuator fixed on the platform. It should be noted that the rotational degree of freedom ψ is kinematically redundant. Indeeed, the platform is designed such that its rotation is a parallelogram mechanism movement, where the tool control point (TCP) is on the neutral axis of this mechanism. Therefore, a rotation ψ of the mobile platform does not induce a movement of the TCP, this is why ψ is permanently maintained at zero. In this work, we are concerned only with the control of the four main actuators of T3KR to perform the pick-and-throw task. Thus, we consider the 4-dimensional coordinate vector $X = [x,y,z,\psi]^T$ as a representation of the pose of the robot's end-effector, and the 4-dimensional coordinate vector $q = [q_1,q_2,q_3,q_4]^T$ as the actuated joint positions. The differential kinematic relationship between the Cartesian and joint velocities can be written as $\dot{X} = J\dot{q}$, where $\dot{X}$ and $\dot{q}$ are the Cartesian and joint velocities, respectively and J is the Jacobian matrix.

2.2 Dynamic modelling of T3KR PKM

Model-based controllers require the inclusion of an accurate dynamic model in the control loop. In order to exploit the dynamic modeling of T3KR robot, the following assumptions often considered in the computation of PKM dynamic model as a good compromise between precision and complexity. (Codourey, 1998):

Assumption 1: *The masses of the forearms are smaller than the other parts of the robot, hence their inertia is neglected.*

Assumption 2: *The mass of each forearm is divided into two point masses located at both extremities of the forearms.*

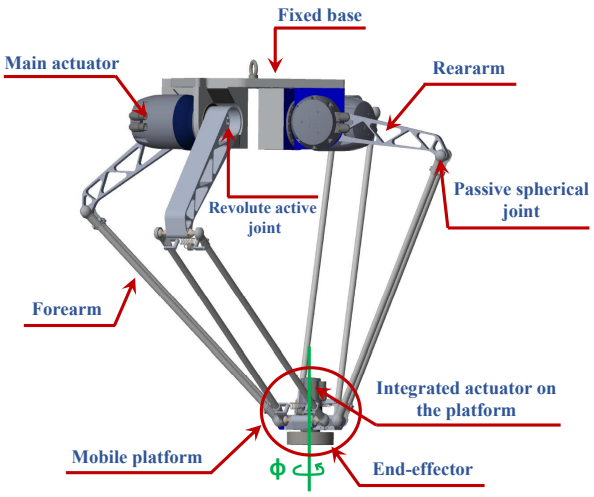

Fig. 1. A CAD View of T3KR PKM with its main components.

Based on the virtual work principle explained in (Bennehar et al., 2018; Escorcia-Hernández et al., 2020b), the dynamics of the T3KR robot can be reduced to the analysis of the dynamics of two main bodies: The moving platform and the main action mechanism consisting of actuators in conjunction with their corresponding rearrarms and forearms. Regarding the moving platform's dynamics, one can define two kinds of forces acting on it induced by gravity and Cartesian accelerations:

$$G_{tp} = -M_{tp}G, \quad F_{tp} = M_{tp}\ddot{X} \tag{1}$$

where $M_{tp} = diag\{m_{tp}, m_{tp}, m_{tp}, i_{tp}\}$ with $m_{tp} = m_n + 4\frac{m_f}{2}$ is the total mass of the moving platform with the half-masses of the forearms. i_{tp} is the total inertia of the mobile platform. $G = [0,0,g,0]^T$ is the gravity vector, being $g = 9.81m/s^2$ the gravity acceleration, and $\ddot{X} \in \mathbb{R}^4$ gives the Cartesian acceleration vector. The contributions of G_{tp} and F_{tp} to actuator torques can be computed by means of the Jacobian matrix $J \in \mathbb{R}^{4\times4}$ as follows:

$$\Gamma_{G_{tp}} = J^T G_{tp}, \quad \Gamma_{F_{tp}} = J^T F_{tp} \tag{2}$$

Regarding the dynamics of the actuators with their corresponding rearrarms and forearms, three contributing torques can be distinguished: (i) the actuators input torque Γ, (ii) the torque contribution of the gravitational forces acting on the rearrarms $\Gamma_{G_{arm}}$, and (iii) the torque contribution of the inertial force acting on the rearrarms Γ_{arm}. The last two ones are denoted as follows:

$$\Gamma_{G_{arm}} = -gM_rCos(q), \quad \Gamma_{arm} = I_{arm}\ddot{q} \tag{3}$$

where $M_r = diag\{m_{req}, m_{req}, m_{req}, m_{req}\}$, being $m_{req} = m_r L_{rG} + L\frac{m_f}{2}$, m_r is the mass of each rearrarm, l_{rG} is the distance from the axis of rotation of each rearrarm to its center of gravity, and L is the complete length of each rearrarm. $Cos(q) = [cos(q_1), cos(q_2), cos(q_3), cos(q_4)]$ where q_i, for $i = 1...4$ are the measured joint positions. We have $I_{arm} = I_{act} + I_r + \frac{L^2 m_f}{2}$, being given that I_{act} and I_r are the actuators inertia and the rearrarm inertia, respectively. The term $\frac{L^2 m_f}{2}$ corresponds to the inertial contribution of the forearms using the second assumption, and $\ddot{q}$ represents the accelerations in joint space.

Table 1. Summary of the main geometric and dynamic parameters of T3KR PKM.

Parameter	Value	Parameter	Value
L (Rearrarm length)	400 mm	m_n (Nacelle mass)	5.68 Kg
l (Forearm length)	900 mm	I_{act} (Actuator inertia)	0.000969 Kg.m^2
m_r (Rearrarm mass)	3.28 Kg	I_r (Rearrarm inertia)	0.173723 Kg.m^2
m_f (Forearm mass)	0.8 Kg		

Following (Codourey, 1998), stating that the sum of all non-inertial forces should be equal to the sum of all inertial forces, and after rearranging the terms, the inverse dynamic model of T3KR robot can be expressed in terms of the joint coordinates q as follows:

$$M(q)\ddot{q} + C(q,\dot{q})\dot{q} + G(q) = \Gamma(t) \tag{4}$$

where $M(q) = I_{arm} + J^T M_{tp} J$ is the total mass and inertia matrix of the robot, $C(q,\dot{q})\dot{q} = J^T M_{tp}\dot{J}$ denotes the Coriolis and centrifugal forces matrix, $G(q) = -\Gamma_{G_{arm}} - \Gamma_{G_{tp}}$ represents the gravitational forces vector, $\Gamma(t)$ is the control input vector. The main geometric and dynamic parameters of T3KR parallel robot are summarized in Table 1.

3. BACKGROUND ON RISE FEEDBACK CONTROL LAW

The dynamics of a n-DOFs kinematic manipulator can be described in joint space as follows Cheng et al. (2003):

$$M(q)\ddot{q} + C(q,\dot{q})\dot{q} + G(q) + F(q,\dot{q}) + D(t) = \Gamma(t) \tag{5}$$

where M, C and G are defined above in (4). $F(q,\dot{q}) \in \mathbb{R}^n$ represents the friction effects vector and $D(t) \in \mathbb{R}^n$ is a general nonlinear disturbances vector (i.e. external disturbances, interaction with the environment, etc).

RISE feedback law is a robust nonlinear strategy that exhibits semi-global asymptotic tracking. This technique includes, in addition to the proportional integral part, a unique integral sign function that constitutes the robustness term of RISE controller. In contrast to many existing robust controllers in the literature, RISE can generate continuous control signals, thus avoiding chattering effects and improving tracking performance. It can compensate for a large class of general uncertainties and external disturbances based on limited assumptions about the disturbances and the controlled system defined as follows (Xian et al., 2004; Bennehar et al., 2018):

Assumption 3: *The inertia matrix $M(q)$ is a symmetric positive-definite matrix satisfying the following inequality bounds for all $\gamma \in \mathbb{R}^n$:*

$$m\|\gamma\|^2 \leq \gamma^T M(q)\gamma \leq \bar{m}(q)\|\gamma\|^2 \tag{6}$$

where m is a known positive constant, $\bar{m}$:$\mathbb{R}_{\geq 0} \to \mathbb{R}_{\geq 0}$ is a non-decreasing function and $\|.\|$ denotes the Euclidean norm of a vector.

Assumption 4: *$C(q,\dot{q})$ and $G(q)$ are bounded if $q(t)$, $\dot{q}(t)$ are bounded and measurable. Moreover, the first two partial derivatives of $M(q)$, $C(q,\dot{q})$, $G(q)$ and $F(q,\dot{q})$ with respect to $q(t)$ and $\dot{q}(t)$ exist and are bounded.*

Assumption 5: *The disturbance vector and its first two time derivatives are bounded (i.e. $D(t), \dot{D}(t), \ddot{D}(t) \in \mathscr{L}_\infty$)*

Assumption 6: *The desired trajectory $q_d(t) \in \mathbb{R}^n$ is differentiable till the 4^{th} order and its derivatives are bounded.*

Let us define the desired joint positions, velocities and accelerations as $q_d(t)$, $\dot{q}_d(t)$, $\ddot{q}_d(t)$, respectively. In order to develop the closed-loop error system, the combined velocity-position tracking error $e_2 \in \mathbb{R}^n$ and the auxiliary filtered tracking error $r \in \mathbb{R}^n$ are denoted as follows:

$$e_2 = \dot{e} + \Lambda_1 e. \tag{7}$$

where $e = q_d - q$ is the output tracking error in joint space. $q_d \in \mathbb{R}^n$ is the desired joint positions and q is the measured one by means of the actuators encoders. $\Lambda_1 \in \mathbb{R}^{n\times n}$ is a diagonal, positive-definite gain matrix.

Based on the closed-loop stability conditions detailed in Xian et al. (2004), RISE feedback control law is given as follows:

$$\Gamma_{RISE} = (K_s + I)e_2(t) - (K_s + I)e_2(t_0) + \int_{t_0}^{t} [(K_s + I)\Lambda_2 e_2(\sigma) + \beta sgn(e_2(\sigma))]d\sigma. \quad (8)$$

where K_s, Λ_2, and $\beta \in \mathbb{R}^{n\times n}$ are positive-definite, diagonal gain matrices, $I \in \mathbb{R}^n$ is identical matrix, t_0 is the initial time and *sgn* is the vector of the sign functions of the combined tracking error. It is worth noting that the second term of the R.H.S of (8) (i.e., $(K_s + I)e_2(t_0)$) is introduced to guarantee a zero control input at time $t = t_0$ (i.e., $\Gamma(t_0) = 0$). For more details about the stability analysis of RISE feedback control, the reader can refer to (Xian et al., 2004).

4. PROPOSED CONTRIBUTION: EXTENDED RISE CONTROL PLUS COMPENSATION

4.1 General Overview on PD Control plus Compensation

Several model-based controllers have already been reported in the introduction, highlighting their improved overall tracking performance compared to non-model-based controllers. The PD plus compensation control law, called PD$^+$, is one of the model-based controllers that is popular in academia. It is a non-adaptive version of the first adaptive controller proposed in 1987 by Slotine and Li, and it is referred to by the names of its creators: "Slotine and Li controller" Slotine and Li (1987); Slotine and Weiping (1988). From a structural point of view, this controller is composed of a PD feedback term plus a compensation term based on the full knowledge of the dynamic model combined with the system state errors. Let us first consider the classical PD control law as follows:

$$\Gamma_{PD} = K_p e(t) + K_d \dot{e}(t) \quad (9)$$

where K_p and $K_d \in \mathbb{R}^+$ are constant feedback gains that are tuned to ensure the stability of the system, and $e(t) = q_d - q$ is the tracking error. Enriching this controller explicitly with the dynamic model of the nonlinear controlled system allows to compensate for uncertainties and parameter variations, and thereby, enhancing the trajectory tracking accuracy. The following equation describes the control law of PD plus compensation:

$$\Gamma_{PD^+} = M(q)(\ddot{q}_d + \alpha\dot{e}(t)) + C(q,\dot{q})(\dot{q}_d + \alpha e(t)) + G(q) + K_p e(t) + K_d \dot{e}(t) \quad (10)$$

where $\alpha \in \mathbb{R}^+$ is defined as: $\alpha = K_d^{-1} K_p$.

4.2 Proposed Extended RISE Control plus Compensation

RISE is a non-model based controller consisting of two main parts: A linear state feedback term similar to a PI controller, depending on the combined tracking error, and a nonlinear robustness term based on the integral of the sign of the combined error. It does not take advantage of knowledge of the manipulator's dynamic model in its control loop. Thus, the dynamic parameter uncertainties and system nonlinearities are not well compensated for by the standard RISE feedback law, especially under critical operating conditions. These issues may lead to high-gain or high-frequency feedback and poor performance in the case of high nonlinearities or in presence of large disturbances. Therefore, to improve the performance of the original RISE controller, we propose to enrich its control structure by adding a full dynamic compensation term. As it can be seen from the equation of PD control plus compensation (10), the compensation term consists of the system dynamic parameters computed online using the measured trajectories and then multiplied by the sum of the desired trajectories with the state errors. To overcome the error resulting from using the desired trajectory signals, RISE control plus compensation is revised by adding a nonlinear auxiliary term depending on the tracking error e_1 and the combined error e_2. This auxiliary term has been added to the Desired Compensation Adaptive law (DCAL) proposed in Sadegh and Horowitz (1990) to compensate for the additional error emerging from using desired trajectories instead of the measured ones in the adaptive feedforward term. The proposed extended RISE control plus compensation, called ERISE$^+$, is expressed as follows:

$$\Gamma_{ERISE^+} = M(q)(\ddot{q}_d + \Lambda_1\dot{e}(t)) + C(q,\dot{q})(\dot{q}_d + \Lambda_1 e(t)) + G(q) + (K_s + I)e_2(t) - (K_s(t_0) + I)e_2(t_0) + \int_{t_0}^{t} \delta\|e(\sigma)\|^2 e_2(\sigma)d\sigma + \int_{t_0}^{t} [(K_{s0} + I)\Lambda_2 e_2(\sigma) + \beta sgn(e_2(\sigma))]d\sigma \quad (11)$$

Based on the stability analysis of the proposed controller, the nonlinear auxiliary term inspired by the DCAL scheme was added with an integral term. Due to space limitation, the stability analysis is not provided in this paper.

5. NUMERICAL SIMULATION RESULTS

In this section, the obtained simulation results of the PD control with computed, the original RISE, proposed ERISE$^+$.

5.1 PD control with computed feedforward

PD control with computed feedforward consists of using the full inverse dynamic model to compensate the effect of nonlinearity but within an offline-computation mode. In fact, the inverse dynamic model is evaluated with the desired trajectories instead of the measured and estimated ones. The joint space control law can be formulated as follows Bennehar (2015):

$$\Gamma_{FFPD} = M(q_d)\ddot{q}_d + C(q_d,\dot{q}_d)\dot{q}_d + G(q_d) + K_p e + K_d \dot{e} \quad (12)$$

where K_p, $K_d \in \mathbb{R}^{n\times n}$ are positive definite diagonal feedback gain matrices. $e(t)$, $\dot{e}(t) \in \mathbb{R}^n$ are the joint position and velocity tracking errors, respectively.

5.2 Pick-and-Throw reference trajectory generation

The reference trajectories, illustrated in Fig. 2, are generated in Cartesian space using a third-order S-curve polynomial motion profile. These generated trajectories correspond to the scenario where the robot has to successively throw three objects of different masses to a target position, $\mathbf{P}_f$, located outside the robot's workspace. First, the robot has to move from the central position $\mathbf{P}_0$ to the first pick position, $\mathbf{P}_1$, to grasp the detected object. Then, and according to the pick and target positions of the corresponding object, a release position $\mathbf{P}_{r_1}$ is calculated.

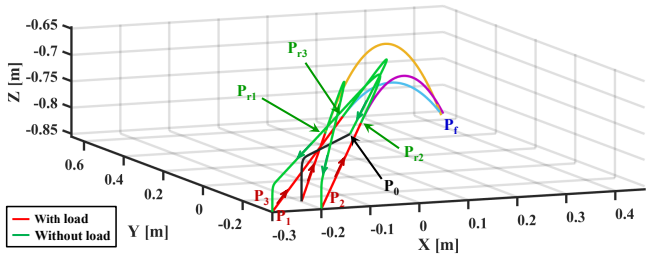

Fig. 2. 3D-view of the P&T reference trajectories of T3KR robot with the ballistic motions of the thrown objects.

After finding the appropriate release point, the robot accelerates to this point (i.e., $\mathbf{P}_{r_1}$), and then throws the object to the desired target $\mathbf{P}_f$. After throwing the object, the robot decelerates to pick the next object, while the released object follows its free flight ballistic trajectory from $\mathbf{P}_{r_1}$ to $\mathbf{P}_f$. The same cyclic movement is repeated for the second and third objects, located respectively at $\mathbf{P}_2$ and $\mathbf{P}_3$. After releasing the last object, the robot returns to its initial position $\mathbf{P}_0$. The whole P&T trajectory is generated taking into account the maximum dynamic performance of the robot (i.e., maximum jerk, acceleration and velocity), the limits of its workspace and the desired target position. Referring to Fig. 2, the red lines represent the portions of the trajectory where the robot carries the object, while the green lines correspond to the portions after the release point where the robot is moving without payload. For more details on the generation of the robot's throw motion with minimum time, the reader can refer to (Hassan et al., 2022).

5.3 Performance evaluation criteria

To quantify the enhancement provided by the proposed ERISE$^+$ controller, we consider the Root Mean Square Error (*RMSE*) criterion for Cartesian translational positions $RMSE_x$ and joint positions $RMSE_q$. These evaluation criteria given by the following equations allow to evaluate the effectiveness of each new control algorithm:

$$RMSE_x = \sqrt{\left(\frac{1}{N}\sum_{i=1}^{N}\left(e_x^2(i)+e_y^2(i)+e_z^2(i)\right)\right)} \tag{13}$$

$$RMSE_q = \sqrt{\left(\frac{1}{N}\sum_{i=1}^{N}\left(e_{q_1}^2(i)+e_{q_2}^2(i)+e_{q_3}^2(i)+e_{q_4}^2(i)\right)\right)} \tag{14}$$

where e_x, e_y and e_z denote the Cartesian position tracking errors along x, y and z *axes*, respectively. e_{q_1}, e_{q_2}, e_{q_3} and e_{q_4} being the joint position tracking errors, and N is the number of samples.

5.4 Control gains tuning procedure

Using the trial and error method, the feedback gains of all the implemented controllers are adjusted. Manually and continuously, we edit the different sets of control gains until the desired performance is obtained. The control gains of the proposed ERISE$^+$ controller are tuned in the same way of those of the original RISE controller using the following procedure: (i) Set $\Lambda_2 = 0$, $\beta = 0$ and $\delta = 0$, (ii) Set Λ_1 and K_s as if it was a PD control plus compensation, where $\Lambda_1(K_s+1)$ is the proportional gain and (K_s+1) is the derivative gain until satisfactory tracking of the reference position and velocity signals is achieved. Then, (iii) start increasing Λ_2 by changing again Λ_1 and K_s either increasing or decreasing until the best possible performance is reached. (iv) Increase β gradually to avoid chattering effects, to improve the robustness of the controller towards disturbances. Finally, (v) increase δ to improve the overall performance while keeping control input torques below saturation. The obtained control gains for the proposed ERISE$^+$, the standard RISE and PD with feedforward controllers are summarized in Table 2.

Table 2. Summary of the feedback control gains.

RISE		**FFPD**	**Proposed ERISE$^+$**	
$\Lambda_1 = 674$	$\beta = 2.5$	$K_p = 2863$	$\Lambda_1 = 150$	$\beta = 2.5$
$\Lambda_2 = 7.2$		$K_d = 22$	$\Lambda_2 = 1.5$	
$K_s = 21$			$K_s = 21$	

5.5 Obtained simulations results

To demonstrate the performance of the proposed ERISE$^+$ controller, a comparative study has been performed with the original RISE and the PD plus feedforward controller through numerical simulations on T3KR robot in a P&T task. This comparison has been established in Matlab/Simulink environment with sampling time of 0.4 ms, using the reference P&T trajectory depicted in Fig.2. Two main scenarios have been implemented on this validation: 1) *scenario 1*: Robustness towards payload changes, 2) *scenario 2*: Robustness towards speed variations. For more realistic simulations, white noise has been added to the output joint positions, coulomb and viscous friction has been added to the dynamic model of the robot as well as a 25% of uncertainty on the inertia value I_{arm} has been considered.

Scenario 1 - Robustness towards payload changes: In this scenario, the maximum operating acceleration was set to 4.2 G. It is the minimum sufficient value required by T3KR robot to throw an object outside of its workspace. The three objects, used for this demonstration, have different masses, which allows to evaluate the robustness of the proposed controller towards variations in payload. The first object has a mass of 50 g, the second one has a mass of 100 g (i.e. $\Delta_{mass} = +100\,\%$ w.r.t the first object), while the third one has a mass of 150 g (i.e. $\Delta_{mass} = +200\,\%$ w.r.t the first object).
The Cartesian tracking errors of the three tested controllers are plotted in Fig. 3. The obtained results clearly show the superiority of the proposed controller over the other two ones along all axes. The RMSE performance indices are evaluated for all controllers, in both Cartesian and joint spaces, and the obtained results are reported in Table 3. According to these indices, the proposed ERISE$^+$ outperforms the standard RISE by 82.7% and 72.6% for the Cartesian and joint spaces, respectively. Compared to the FFPD control, the proposed ERISE$^+$ improves the tracking performance by up to 50.3% and 45.9% in the Cartesian and joint spaces, respectively.
The evolution of the generated control input torques for all controllers is displayed in Fig. 4. The control signals show, for all controllers, a good and smooth behavior within the admissible limits of the actuators of the robot (the maximum torque of T3KR actuators is 28.9 N.m). In addition, a slight reduction in energy consumption is notified for the proposed ERISE$^+$ controller compared to the two other controllers.
This scenario confirms the effectiveness of the proposed controller compared to the standard RISE and FFPD controllers. The proposed ERISE$^+$ control scheme is more robust towards

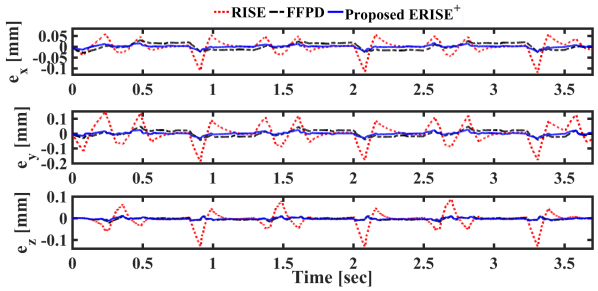

Fig. 3. Scenario 1: Evolution of the Cartesian tracking errors versus time.

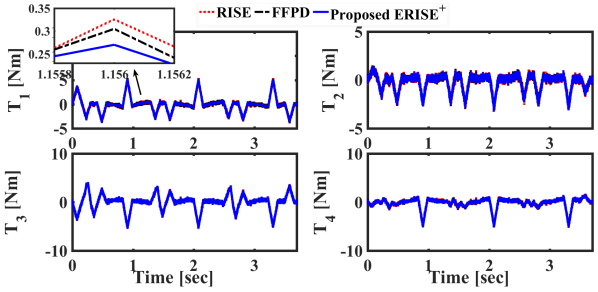

Fig. 4. Scenario 1: Evolution of the control input torques versus time.

variations in payload, thus, it is more suitable for arbitrary P&T applications such as waste sorting.

Scenario 2 - Robustness towards speed variations: The T3KR robot is intended to be used for high-speed P&T sorting applications. Accordingly, it is useful to evaluate the tracking performance of the proposed ERISE$^+$ strategy at high-acceleration conditions. The operating acceleration is increased up to 9 G. In this scenario, the robot performs the same P&T trajectory with the same manipulated objects as in the previous scenario.

In Fig. 5, one can obviously see the significant improvements obtained by the proposed ERISE$^+$ control scheme along all translational axes. These improvements are quantified by exploiting the RMSE evaluation criteria in Cartesian and joint spaces. The obtained results, summarized in Table 3, show improvements of 81.4% in the Cartesian space and 71.1% in the joint space compared to the standard RISE controller. In comparison to the FFPD control law, the tracking performance is improved by up to 31.3% and 28.7% in the Cartesian and joint spaces, respectively.

The evolution of the control input torques, generated by the three controllers, are depicted in Fig. 6. It can be seen that all the control signals are continuous and evolve within the admissible range of the actuators' capabilities. Moreover, as shown in Fig. 6, the proposed controller slightly reduces the power consumption as it generates less input torques, compared to the standard RISE and FFPD controllers.

The overall performance improvement, obtained by the proposed ERISE$^+$ scheme, can be explained by the good compensation of the system nonlinearities provided by the contribution of the designed compensation dynamic term.

6. CONCLUSION AND FUTURE WORK

The main contribution of this work is a new category of RISE control strategy applied to PKMs. RISE is a non-model based

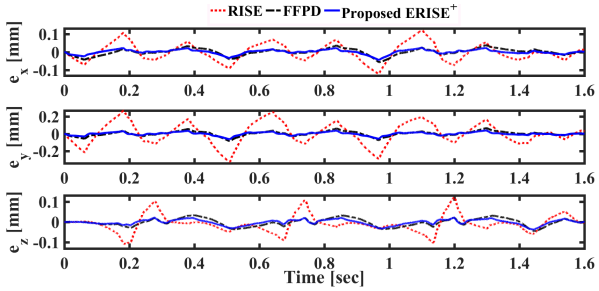

Fig. 5. Scenario 2: Evolution of the Cartesian tracking errors versus time.

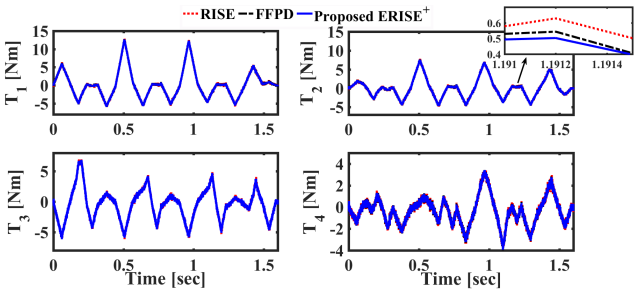

Fig. 6. Scenario 2: Evolution of the control input torques versus time.

controller that provides semi-global asymptotic tracking of the reference trajectory under certain limitations of the system dynamics and external disturbances. We proposed to add a nonlinear model-based compensation term inspired by PD control with compensation. The compensation term consists of dynamic parameters calculated online and multiplied by the sum of the desired trajectories with state errors. To overcome the error resulting from the use of desired joint accelerations and velocities, the resulting controller is extended by a nonlinear auxiliary function based on the tracking error. The standard RISE control, PD plus feedforward and the proposed extended RISE control with compensation have been implemented through numerical simulations on the T3KR parallel robot. The obtained results clearly show the superiority of the proposed controller over the other two controllers in terms of tracking accuracy and robustness w.r.t. payload and velocity changes. This work can be extended with the stability analysis of the proposed controller as well as its validation in real-time experiments. In addition, the dynamic parameters of the manipulator may vary over time or be unknown, thus, a real-time estimation of these modeled parameters may be considered to further improve its tracking performance.

Table 3. Summary of the obtained tracking performances.

Scenario	Control	$RMSE_x$[mm]	$RMSE_J$[deg]
Scenario 1	RISE	0.0736	0.0073
	FFPD	0.0256	0.0037
	Proposed ERISE$^+$	0.0127	0.0020
	IMP w.r.t RISE	**82.7 %**	**72.6 %**
	IMP w.r.t FFPD	**50.3 %**	**45.9 %**
Scenario 2	RISE	0.1393	0.0180
	FFPD	0.0377	0.0073
	Proposed ERISE$^+$	0.0259	0.0052
	IMP w.r.t RISE	**81.4 %**	**71.1 %**
	IMP w.r.t FFPD	**31.3 %**	**28.7 %**

ACKNOWLEDGEMENTS

This work is supported by Tecnalia "Pick-and-Throw" research project. The corresponding author acknowledged the Lebanese University and the social foundation AZM and SAADE for financial support.

REFERENCES

Bennehar, M. (2015). *Some contributions to nonlinear adaptive control of PKMs: from design to real-time experiments*. Ph.D. thesis.

Bennehar, M., Chemori, A., Bouri, M., Jenni, L.F., and Pierrot, F. (2018). A new rise-based adaptive control of pkms: design, stability analysis and experiments. *International Journal of Control*, 91(3), 593–607.

Bennehar, M., Chemori, A., Pierrot, F., and Creuze, V. (2015). Extended model-based feedforward compensation in 1 adaptive control for mechanical manipulators: Design and experiments. *Frontiers in Robotics and AI*, 2, 32.

BHS (2018). Max-AI AQC robotic sorter. *https://www.youtube.com/watch?v=2gjUpDnJrZA*.

Cheng, H., Yiu, Y.K., and Li, Z. (2003). Dynamics and control of redundantly actuated parallel manipulators. *IEEE/ASME Transactions on mechatronics*, 8(4), 483–491.

Clavel, R. (1990). Device for the movement and positioning of an element in space. URL `https://patents.google.com/patent/US4976582A`.

Codourey, A. (1998). Dynamic modeling of parallel robots for computed-torque control implementation. *The International Journal of Robotics Research*, 17(12), 1325–1336.

Dalvand, M.M. and Shirinzadeh, B. (2012). Remote centre-of-motion control algorithms of 6-rrcrr parallel robot assisted surgery system (pramiss). In *2012 IEEE International Conference on Robotics and Automation*, 3401–3406. IEEE.

Escorcia-Hernández, J.M., Aguilar-Sierra, H., Aguilar-Mejia, O., Chemori, A., and Arroyo-Nuñez, J.H. (2020a). A new adaptive rise feedforward approach based on associative memory neural networks for the control of pkms. *Journal of Intelligent & Robotic Systems*, 100(3), 827–847.

Escorcia-Hernández, J.M., Chemori, A., Aguilar-Sierra, H., and Monroy-Anieva, J.A. (2020b). A new solution for machining with ra-pkms: Modelling, control and experiments. *Mechanism and Machine Theory*, 150, 103864.

Feemster, M. (2014). Jitter reduction in a directed energy application using rise. In *2014 American Control Conference*, 2451–2455. IEEE.

Fischer, N., Bhasin, S., and Dixon, W. (2011). Nonlinear control of an autonomous underwater vehicle: A rise-based approach. In *Proceedings of the 2011 American Control Conference*, 3972–3977. IEEE.

Grange, S., Conti, F., Helmer, P., Rouiller, P., and Baur, C. (2001). Overview of the delta haptic device. Technical report.

Hassan, G., Chemori, A., Chikh, L., Hervé, P.E., El Rafei, M., Francis, C., and Pierrot, F. (2020). Rise feedback control of cable-driven parallel robots: Design and real-time experiments. In *1st Virtual IFAC World Congress (IFAC-V)*.

Hassan, G., Gouttefarde, M., Chemori, A., Hervé, P.E., El Rafei, M., Francis, C., and Sallé, D. (2022). Time-optimal pick-and-throw s-curve trajectories for fast parallel robots. *IEEE/ASME Transactions on Mechatronics*.

Kelly, R. (1997). Pd control with desired gravity compensation of robotic manipulators: a review. *The International Journal of Robotics Research*, 16(5), 660–672.

Kelly, R., Davila, V.S., and Perez, J.A.L. (2006). *Control of robot manipulators in joint space*. Springer Science & Business Media.

Merlet, J.P. (2006). *Parallel robots*, volume 128. Springer Science & Business Media.

Natal, G.S., Chemori, A., and Pierrot, F. (2014). Dual-space control of extremely fast parallel manipulators: Payload changes and the 100g experiment. *IEEE Transactions on Control Systems Technology*, 23(4), 1520–1535.

Raptopoulos, F., Koskinopoulou, M., and Maniadakis, M. (2020). Robotic pick-and-toss facilitates urban waste sorting. In *2020 IEEE 16th International Conference on Automation Science and Engineering (CASE)*, 1149–1154. IEEE.

Ren, L., Mills, J.K., and Sun, D. (2007). Experimental comparison of control approaches on trajectory tracking control of a 3-dof parallel robot. *IEEE Transactions on Control Systems Technology*, 15(5), 982–988.

Sadegh, N. and Horowitz, R. (1990). Stability and robustness analysis of a class of adaptive controllers for robotic manipulators. *The International Journal of Robotics Research*, 9(3), 74–92.

Saied, H., Chemori, A., Bouri, M., El Rafei, M., Francis, C., and Pierrot, F. (2019). A new time-varying feedback rise control for second-order nonlinear mimo systems: theory and experiments. *International Journal of Control*, 1–14.

Shang, W.W., Cong, S., Li, Z.X., and Jiang, S.L. (2009). Augmented nonlinear pd controller for a redundantly actuated parallel manipulator. *Advanced Robotics*, 23(12-13), 1725–1742.

Shang, W. and Cong, S. (2009). Nonlinear computed torque control for a high-speed planar parallel manipulator. *Mechatronics*, 19(6), 987–992.

Sherwani, K.I., Kumar, N., Chemori, A., Khan, M., and Mohammed, S. (2020). Rise-based adaptive control for eicosi exoskeleton to assist knee joint mobility. *Robotics and Autonomous Systems*, 124, 103354.

Slotine, J.J. and Weiping, L. (1988). Adaptive manipulator control: A case study. *IEEE transactions on automatic control*, 33(11), 995–1003.

Slotine, J.J.E. and Li, W. (1987). On the adaptive control of robot manipulators. *The international journal of robotics research*, 6(3), 49–59.

Slotine, J.J.E., Li, W., et al. (1991). *Applied nonlinear control*, volume 199. Prentice hall Englewood Cliffs, NJ.

Stewart, D. (1965). A platform with six degrees of freedom. *Proceedings of the institution of mechanical engineers*, 180(1), 371–386.

Wen, S., Qin, G., Zhang, B., Lam, H.K., Zhao, Y., and Wang, H. (2016). The study of model predictive control algorithm based on the force/position control scheme of the 5-dof redundant actuation parallel robot. *Robotics and Autonomous Systems*, 79, 12–25.

Xian, B., Dawson, D.M., de Queiroz, M.S., and Chen, J. (2004). A continuous asymptotic tracking control strategy for uncertain nonlinear systems. *IEEE Transactions on Automatic Control*, 49(7), 1206–1211.

Yao, J., Jiao, Z., and Ma, D. (2014). Rise-based precision motion control of dc motors with continuous friction compensation. *IEEE Transactions on Industrial Electronics*, 61(12), 7067–7075.